ELSEVIER

Applied Catalysis A: General 159 (1997) 171–185

Oxidative coupling of methane over BaF_2-promoted rare earth oxides with variable valence

Ruiqing Long, Jizhong Luo, Mingxin Chen, Huilin Wan*

Department of Chemistry and State Key Laboratory for Physical Chemistry of the Solid Surface, Xiamen University, Xiamen 361005, China

Received 30 September 1996; received in revised form 22 January 1997; accepted 29 January 1997

Abstract

The catalytic behaviors for oxidative coupling of methane (OCM) over BaF_2-promoted CeO_2, Pr_6O_{11} and Tb_4O_7 catalysts have been studied. It was found that methane conversion, C_2 selectivities and C_2H_4/C_2H_6 ratio over the BaF_2-promoted catalysts were significantly higher than those over the corresponding oxides. The maximum C_2 selectivity (37.5%) and yield (19.5%) were obtained over the BaF_2/Pr_6O_{11} (BaF_2=2) catalyst under the conditions of 1073 K, CH_4/O_2=7:1 and GHSV=60 000 h^{-1}. XRD analysis indicated that partial ion exchange took place during the catalyst preparation, leading to the generation of BaF_2 hence under the formation of rare earth oxyfluorides. XRD, XPS and TPR measurements revealed that the concentration of specific lattice oxygen species increased after adding BaF_2 to the rare earth oxides. This will be favorable to decreasing the chance of deep oxidation of methyl radicals and C_2 hydrocarbons and therefore result in an increase of C_2 selectivity. Since there is a certain correlation between methane conversion and C_2 selectivity for an oxygen-limited OCM reaction, methane conversion will also be found to increase along with the increase of C_2 selectivity. However, no direct relationship between the surface oxygenicity and catalytic activity/selectivity was observed over these catalysts.

Keywords: Methane; Oxidative coupling; Rare earth oxides; BaF_2; Ion exchange

1. Introduction

The oxidative coupling of methane (OCM) to ethane and ethene is an attractive reaction to convert natural gas into valuable chemicals. Since the pioneering work by Keller and Bhasin [1], OCM has become a subject of intense research world-

* Corresponding author.

PII S0926-860X(97)00043-1

wide in recent years. Almost all elements in the periodic table have been studied as OCM catalysts [2]. In rare earth oxide OCM catalysts, La_2O_3, Nd_2O_3 and Sm_2O_3 have been extensively studied due to their high catalytic activities and selectivities as well as satisfactory thermal stabilities [3–6]. However, poor C_2 selectivities were obtained over CeO_2, Pr_6O_{11}, and Tb_4O_7 [3,4,7] due to their high oxidation reactivities to methyl radicals [4]. In order to improve the catalytic performance of these oxidative rare earth oxides for OCM reaction, some promoters, usually alkali-metal [7–9] or chlorine [10], have been added to these oxides. Pointer et al. [8] observed that the addition of Li to PrO_x resulted in an improvement in C_2 selectivity, with a decrease in methane conversion. They ascribed the change of catalytic performance to the formation of a mixed carbonate layer, which decreased the concentration of labile oxygens on a praseodymium oxide surface, after adding lithium to praseodymium oxide. Fujiyama et al. reported that over La_2O_3, Pr_6O_{11}, and Sm_2O_3, addition of a small amount of tetrachloroethane to the reactant stream improved the catalytic activity. The improvement of the activity was primarily due to the formation of the oxychlorides during the reaction [10]. Metal fluorides have been found to have significant promotional roles on some oxide catalysts for the OCM and oxidative dehydrogenation of light alkanes (C_2H_6 and C_3H_8) reactions [11–14]. We reported previously that adding various content of BaF_2 to CeO_2 improved apparently C_2 selectivity and yield for OCM reaction [13]. In order to investigate the nature of the promoting effect of BaF_2, we have further studied the catalytic performance for OCM over the other two oxidative rare earth oxides promoted by BaF_2. The present work is mainly concerned with the catalytic performance over the BaF_2-promoted oxidative CeO_2, Pr_6O_{11} and Tb_4O_7 catalysts and, in particular, with the correlations between the catalytic performance of these materials and their bulk and surface properties, as characterized by X-ray diffraction (XRD), X-ray photoelectron spectroscopy (XPS), temperature program desorption (TPD) and temperature program reduction (TPR) characterizations.

2. Experimental

2.1. Preparation and evaluation of catalysts

The catalysts were prepared by the method of grinding and calcining, as described elsewhere [14]. The solid mixture was mixed with a certain content of deionized water to form a paste, followed successively by drying at 393 K for 4 h and calcining at 1173 K for 6 h. The resulting solid was crushed and sieved to 40–60 mesh particles. The pure CeO_2 (≥99.5%), Pr_6O_{11} (≥99.9%), Tb_4O_7 (99.95%) and BaF_2 used for the catalytic performance evaluation were also treated with procedures similar to those as described above. The other reagents used in the preparation were all analytical grade.

The catalytic reaction was carried out in a fixed-bed quartz microreactor (5.0 mm I.d.), under the conditions of CH_4/O_2=3 (mole ratio, without dilution gas) and GHSV=20 000 h^{-1}. Methane (99.99%) and oxygen (99.5%) were used without further purification. In each experimental run, 0.20 ml of catalyst was used; the effluent gas was analyzed at room temperature by an on-line Shimadzu 102GD gas-chromatograph equipped with thermal conductivity detector. Water and hydrogen were also present but were not monitored. Other details were the same as reported previously [14].

3.2. Characterization of catalyst

The specific surface area of the catalyst was measured by BET method with N_2 adsorption at 77 K on a Sorptomatic 1900 CARLOERBA instrument. A large amount of catalyst (5.0 g) was used in order to increase the precision of the measurement. The samples were outgassed at 523 K in vacuum (5×10^{-2} Torr, 1 Torr=133.3 N/m^2) for 3 h before N_2 adsorption.

XRD experiment was carried out at room temperature on a Rigaku Rotaflex D/Max-C system with Cu K_α (λ=0.15406 nm) radiation. The samples were loaded to a depth of 1 mm on a sample holder. XRD powder patterns were recorded in the range of 2θ=20–70°.

The surface composition was analyzed by means of XPS. Spectra were recorded on a VG ESCALAB 210 XPS/AES instrument at room temperature, with Mg K_α (for the samples containing Co or Pt) or Al K_α (for the samples containing Tb) as the excitation radiation. The catalyst samples were pressed into wafers (Ø10 mm) under the pressure of 100 kgf/cm^2 and were loaded on a sample holder for XPS analysis. The base pressure of the XPS analysis chamber was about 7×10^{-11} Torr. All measured binding energies were calibrated with respect to the C 1s energy at 284.6 eV, due to adventitious carbon. Eclipse 1.7T software was used to resolve the experimental spectra. The surface compositions of the catalysts were estimated from peak areas using appropriate instrumental sensitivity factors.

The acidity and basicity of the catalysts were measured by TPD of pyridine (Py) and carbon dioxide (adsorbed at 300 K), respectively, in a quartz microreactor from 300 to 1173 K, at a linear heating rate of 20 K/min in a flow of helium (30 ml/min). Before the TPD experiment, the catalyst (0.2 g) packed in a quartz reactor was treated in a flow of helium at 1175 K for 30 min. The desorbed pyridine and carbon dioxide were detected by a gas chromatograph equipped with a thermal conductivity detector.

Each TPR experiment was carried out in a quartz microreactor. 11% H_2/Ar at a flow rate of 15 ml/min was used as a reducing gas. In each of the experiments, the sample (80–100 mesh) was subjected to TPR from 298 to 1223 K at a heating rate of 20 K/min. A thermal conductivity detector was used for this purpose. The effluent gas was purified with KOH and 5A molecular sieve columns to get rid of H^2 (which may be produced on the RuF_3-promoted samples

during the TPR experiment) and H_2O before it got into the thermal conductivity detector.

3. Results and discussion

3.1. Catalytic performance evaluation

The catalytic performance evaluations of the catalysts are summarized in Table 1. Under the conditions of 1073 K, CH_4:O_2=3:1 and GHSV=20 000 h^{-1}, pure CeO_2, Pr_6O_{11} and Tb_4O_7 showed relatively high activities to methane, but the C_2 selectivities were very low, the major products were CO and CO_2. This result is similar to the previous studies [3,4,7,15]. Over the undiluted rare earth oxides, the C_2 selectivities decreased with the sequence of Tb>Pr>Ce, which was consistent with the increase of bulk Ln^{4+} (Ln=Ce, Pr, Tb) concentrations in the catalysts. When BaF_2, which gave a poor activity for OCM [12], was added to these oxides, C_2 selectivities were found to improve markedly, at the same time, CH_4 conversions and C_2H_6/C_2H_4 ratios were also measured under identical conditions, leading to an apparent increase in C_2 yields and, particularly, in C_2H_4 yields. The C_2 selectivities and yields were found to increase according to the sequence of BaF_2/Pr_6O_{11} (Ba/Pr=2)>BaF_2/Tb_4O_7 (Ba/Tb=2)>BaF_2/CeO_2 (Ba/Ce=4) under the same conditions. The maximum C_2 selectivity (57.5%) and yield (19.3%) were obtained over the BaF_2/Pr_6O_{11} catalyst. In addition, the ratios of CO/CO_2 were very low (<0.1) on the BaF_2-promoted catalysts, which might be attributed to the rapid surface reactions in which methyl radicals and/or CO were deeply oxidized to CO_2.

Regardless of whether the catalysts were promoted by BaF_2 or not, the conversions of oxygen were more than 99%, which suggested that the OCM reaction was carried out under an oxygen-limited condition. This makes it difficult to compare the real activities of these catalysts: the reason for the increase in methane conversion becomes complex as a result of adding BaF_2 to these rare earth oxides with variable valences. It is interesting to note that, for all of the catalysts, the

Table 1
The catalytic performance evaluations and specific surface areas of the catalysts

Catalyst	Conv. (%)		Selectivity (%)			C_2H_6/C_2H_4	C_2 Yield (%)	Surface area (m^2/g)
	CH_4	O_2	CO	CO_2	C_2			
CeO_2	22.4	99.6	31.3	23.8	2.8	0.83	0.6	4.1
BaF_2/CeO_2 (Ba/Ce=4)	32.5	99.5	2.3	45.2	36.6	1.7	17.6	2.5
Pr_6O_{11}	23.1	99.5	8.0	31.5	21.6	0.64	5.0	4.9
BaF_2/Pr_6O_{11} (Ba/Pr=2)	33.6	99.4	3.7	20.8	37.5	1.6	19.3	2.3
Tb_4O_7	28.8	99.5	10.0	47.1	23.5	0.89	5.3	3.7
BaF_2/Tb_4O_7 (Ba/Tb=2)	30.1	99.4	3.9	30.0	36.1	1.7	18.6	3.1

Conditions: T=1073 K, CH_4/O_2=3/1 (mixture diluted gas) and GHSV=20 000 h^{-1}.

higher the C_2 selectivity, the higher the methane conversion under the same conditions (Table 1). So it is suggested that C_2 selectivity may have something to do with methane conversion for an oxygen-limited OCM reaction. It is noted that the amount of oxygen consumed in converting a definite amount of methane to ethene and ethane is smaller than that in converting the same amount of methane to CO_x ($CO+CO_2$). For an oxygen-limited OCM reaction, there will be little oxygen left in the gas phase after flowing over a short distance of the catalyst bed, and thus a large amount of methane cannot be converted any longer. Due to the increase in C_2 selectivity as a result of adding BaF_2 to the multivalent rare earth oxides, a smaller amount of oxygen would be used up in converting the same definite amount of methane (mainly to C_2 products) over the BaF_2-promoted catalysts than that over pure oxides (mainly to CO_x). This led to the results that the conversion zones of the catalyst bed for the further catalytic reaction appeared to be longer, and methane conversions were higher, than those for the latter catalysts. At the same time, with the increase of the length of catalyst bed being exposed to gaseous oxygen, the chance that ethene reacts with surface active oxygen species to produce ethene will increase, resulting in an improvement in ethene-to-ethane ratio over the BaF_2-promoted catalysts, as compared with the corresponding pure oxides.

3.2. Bulk phase composition and structure

The XRD results (Table 2) showed that pure CeO_2, Pr_6O_{11} and Tb_4O_7 were cubic. In the fresh BaF_2/CeO_2 (Ba/Ce=4) catalyst, only cubic BaF_2 (a=6.172) and CeO_2 were found; while, in the fresh BaF_2/Tb_4O_7 (Ba/Tb=2) catalyst, besides cubic BaF_2 (a=6.184) and Tb_4O_7, a new rhombohedral TbOF phase formed. Cubic BaF_2 (a=6.134) and rhombohedral PrOF were also detected in the fresh BaF_2/Pr_6O_{11} (Ba/Pr=2) catalyst, but cubic $PrO_{1.83}$ was not found by XRD. These results reveal that the contents of Ln^{4+} (Ln=Ce, Pr, Tb) in these catalysts decrease according to the sequence of BaF_2/CeO_2>BaF_2/Tb_4O_7>BaF_2/Pr_6O_{11}. As compared with pure BaF_2 lattice (a=6.200), the BaF_2 lattice in the above catalysts slightly contracted. This may result either from partial substitution of the Ba^{2+} (r=0.134 nm) in BaF_2 lattice by Ln^{3+} (r_{Pr}=0.1013 nm, r_{Tb}=0.0923 nm) or

Table 2
The bulk composition and structure of the fresh catalysts

Catalyst	Composition and structure[a]
CeO_2	Cubic CeO_2
BaF_2/CeO_2 (Ba/Ce=4)	Cubic CeO_2 (s), cubic BaF_2 (s, a=6.172)
Pr_6O_{11}	Cubic $PrO_{1.83}$
BaF_2/Pr_6O_{11} (Ba/Pr=2)	Cubic BaF_2 (w, a=6.134), rhombohedral PrOF (w)
Tb_4O_7	Cubic Tb_4O_7
BaF_2/Tb_4O_7 (Ba/Tb=2)	Cubic Tb_4O_7 (w), cubic BaF_2 (s, a=6.184), rhombohedral TbOF (vw)

[a] s=strong, w=medium, vw=weak, vvw=very weak.

Ln^{4+} (r_{Ce}=0.092 nm, r_{Pr}=0.090 nm, r_{Tb}=0.084 nm), or from partial replacement of the F^- by O^{2-}, leading to the formation of more anionic vacancies in the lattice. These results suggest that the partial ion exchange had happened in the process of catalyst preparation, leading to the contraction of BaF_2 lattice and/or the formation of oxyfluorides. Taking into account that no oxyfluoride phase formed in the BaF_2/CeO_2 catalyst and the content of oxyfluoride in the BaF_2/Pr_6O_{11} was more than that in the BaF_2/Tb_4O_7 (Table 2), one can infer that the exchange extent between F^- and O^{2-} ions in the catalysts increased in the order of Ce<Tb<Pr. Due to the fact that the conductivities of these rare earth oxides with variable valence increase with the sequence of Ce<Tb<Pr at high temperature [16], the mobilities of lattice oxygen may also increase in this order. For those oxides with higher mobility of lattice oxygen, the anionic exchange between them and BaF_2 at high temperature might be easier.

Cubic CeO_2 is a compound with fluorite structure. Cubic Pr_6O_{11} ($PrO_{1.83}$) molecule may be thought as made up of four PrO_2 and one Pr_2O_3. Similarly, cubic Tb_4O_7 molecule is also made up of two TbO_2 and one Tb_2O_3. The cubic LnO_2 is a fluorite-type structure and the structure of cubic Ln_2O_3 is closely similar to that of the fluorite but with 1/4 intrinsic oxygen vacancies [17], so it is reasonable to conclude that a considerable number of anionic vacancies exist in cubic Pr_6O_{11} and Tb_4O_7 lattice. The structure of rhombohedral LnOF [18], whose chemical composition is rigorously defined, is a slightly distorted fluorite-type structure. Considering that many compounds with fluorite-type structure, e.g. alkaline–earth fluorides, have anion Frenkel defects and anionic vacancies [19], one can infer that the similar anionic vacancies may also exist in the oxyfluoride compounds with fluorite-like structure. On the other hand, the ionic exchange between the oxide and fluoride phases in the catalysts may also lead to the formation of more anionic vacancies in order to maintain electroneutrality. The presence of anionic vacancies in the above catalysts will be beneficial to the adsorption and activation of O_2 under the reaction conditions.

Comparing the concentration of Ln^{4+} in the catalysts with C_2 selectivity for OCM (Table 1), one can find that C_2 selectivity increases with the decrease of the concentration of Ln^{4+}. Since the multivalent rare earth oxides have high reactivity to methyl radicals due to the rapid interconversion of oxidation states (Ln^{3+}/Ln^{4+}) and rapid diffusion of O_2 in the bulk [7], the addition of BaF_2 to Pr_6O_{11} and Tb_4O_7 leads to the formation of oxyfluorides, which stabilize the Ln^{3+} oxidation state and suppress the Ln^{4+} ions that are associated with the labile oxygens responsible for surface total oxidation of methane and C_2 hydrocarbons. This will be favorable to the increase of C_2 selectivity.

3.3. Surface composition

The electron binding energies (BE) and surface compositions of the elements on the fresh catalysts as measured by XPS are summarized in Tables 3 and 4.

Table 3
Electron binding energies of the elements in the fresh catalysts as measured by XPS

Catalyst	Binding energy (eV)					
	Ce $3d_{5/2}$ or $4d_{5/2}$	Ba $3d_{5/2}$	F 1s	O 1s	C 1s	
CeO_2	882.3	—	—	532.8, 531.3, 529.3	289.0, 284.6	
BaF_2/CeO_2 (Ba/Ce=4)	891.5	780.9	684.3	531.9, 530.4, 528.9	288.2, 284.8	
Pr_6O_{11}	934.9, 933.3	—	—	531.3, 529.5, 528.9	288.6, 284.6	
BaF_2/Pr_6O_{11} (Ba/Pr=2)	935.0, 933.3	780.6	684.4	531.8, 530.5, 528.6	288.6, 284.8	
Tb_4O_7	1152.9, 1152.7	—	—	531.5, 529.7, 528.8	288.6, 284.6	
BaF_2/Tb_4O_7 (Ba/Tb=2)	1157.7, 1156.0	780.6	684.4	531.7, 530.3, 528.3	288.3, 284.6	

[a] $3d_{5/2}$ BE for Ce and Pr; $4d_{5/2}$ BE for Tb.

Table 4
Surface composition of various elements in the fresh catalysts

Catalyst	surface concentration (C_s, at%)							
	Ce^{4+}	Ce^{3+}	Ba^{2+}	F^-	O^{2-}	Other oxygen[b]	C^*	Ba/Ce
CeO_2	4.1	trace	—	—	34.7	57.7	3.5	—
BaF_2/CeO_2 (Ba/Ce=4)	1.3	trace	20.8	28.3	18.6	28.3	3.0	16.1
Pr_6O_{11}	2.8	3.3	—	—	50.7	30.9	7.4	—
BaF_2/Pr_6O_{11} (Ba/Pr=2)	1.4	2.2	20.9	48.1	8.5	18.8	2.1	5.8
Tb_4O_7	16.3	6.3	—	—	41.6	33.7	3.0	—
BaF_2/Tb_4O_7 (Ba/Tb=2)	6.4	2.6	23.7	30.5	11.2	21.9	2.8	2.6

[a] C_s=(A/S)/(E/A/S), atomic sensitivity factor.
[b] Other oxygen refers to the oxygen CO_3^{2-}, OH^-, O^-, O_2^{2-} and O_2^-.
[c] C from the surface contamination.

respectively. In the C 1s spectra, besides the carbon peak due to adventitious carbon at 284.6 eV, another peak is observed at higher energy (288.2–289.0 eV) on the catalysts, which corresponds typically to a carbon atom belonging to a carbonate group [20]. All of the O 1s spectra in the catalysts could be resolved to three peaks located at ca. 531.9, 530.5 and 528.7 eV, respectively (Table 3). The peaks at ca. 528.7 eV can be attributed to lattice oxygen (O^{2-}) [21,22], while the other peaks at ca. 531.9 and 530.5 eV cannot be identified because the BE values of some oxygen species fall in the range of 530–535 eV. Since the ratios of these oxygen atomic concentrations to carbon atomic concentrations with higher C 1s BE were far more than 3, it can be believed that other oxygen species, e.g. OH^-, O_2^{2-}, O^- and O_2^-, may also exist on the surface of the catalysts besides CO_3^{2-} [20–24]. The O_2^{2-} and O_2^- adspecies formed on the surface of CeO_2 and BaF_2/CeO_2 catalysts have been proved by in situ microprobe Raman spectroscopy in our previous studies [25,26].

In the Ce $3d_{5/2}$ spectrum of CeO_2, only a peak with BE 882.3 eV due to Ce^{4+} [20] was detected. The addition of BaF_2 to cerium oxide led to the results that the

concentration of Ce^{4+} decreased and the Ce $3d_{5/2}$ BE value shifted to lower energy. Zhou et al. ascribed the decrease of the BE to the formation of quasi-free electrons around Ce^{4+} or the presence of a partially reduced state of Ce^{3+} ion [13]. The Pr $3d_{5/2}$ spectrum for Pr_6O_{11} displayed a broad signal. It could be resolved to two peaks with BE of ca. 934.9 and 933.1 eV, which could be assigned to quadrivalent and trivalent praseodymium ions, respectively [20]. A small amount of Pr^{4+} and Pr^{3+} ions were also observed on the BaF_2/Pr_6O_{11} catalyst surface (Table 3, Table 4), although no Pr_6O_{11} phase was found in the catalyst bulk according to the above XRD result. In the case of $TbCl_4O_7$ and BaF_2/Tb_4O_7, Tb 4d BE were used to distinguish between Tb^{4+} and Tb^{3+} ions because Tb^{4+} and Tb^{3+} ions have a close $3d_{5/2}$ BE [20]. Two peaks at 149.4 and 146.7 eV due to Tb^{4+} and Tb^{3+}, respectively, were detected on the surface of the Tb_4O_7 sample. Tb^{4+} and Tb^{3+} ions were also observed on the BaF_2/Tb_4O_7 surface, but their concentrations were lower than those of the Tb_4O_7 sample. On all the BaF_2-promoted catalysts, Ba^{2+} and F^- ions were detected, and the Ba/Ln (Ln=Ce, Pr, Tb) ratios on the surface were apparently higher than those in the bulk. This indicates an enrichment of the surface in barium.

The above XPS results indicated that the addition of BaF_2 to the rare earth oxides with variable valence decreased the concentrations of the surface quadrivalent rare earth ions, but this phenomenon was less apparent than that in the bulk (XRD results). This may be attributed to the fact that the catalyst surface is more complex than the bulk, where partial rare earth ions with lower valence may also be changed to higher valence ions due to the adsorption and activation of gaseous oxygen. As described in the XRD part, the decrease in the concentration of surface quadrivalent ions will be beneficial to the improvement of C_2 selectivity for OCM. On the other hand, the dispersion of F^- on the surface of catalyst will also be helpful for the isolation of the surface active centers and thus will decrease the chance of deep oxidation of methyl radicals and C_2 hydrocarbons.

3.4. Surface area and surface acidity and basicity

From Table 1, one can see that all of the specific surface areas of the BaF_2-promoted multivalent rare earth oxides were smaller than those of the corresponding oxides. Since a methyl radical will collide with a catalyst surface about 10^3 times before it can efficiently couple with another methyl radical to form an ethane molecule in the gas phase [27], the decrease of specific surface area as a result of adding BaF_2 to these oxides may also lead to a decrease in porosity of the catalyst and thus a decreasing extent of diffusion control for such a fast radical reaction, resulting in an increased selectivity of C_2 hydrocarbons.

The Py–TPD spectra from the catalyst surface are shown in Fig. 1. Three Py desorption peaks occurring at 393, 501 and 1068 K over the CeO_2 catalyst, which are assigned to the weak, intermediate and strong acidic sites, respectively. The TPD result of Py-adsorbed Pr_6O_{11} showed the existence of four peaks at 383, 583,

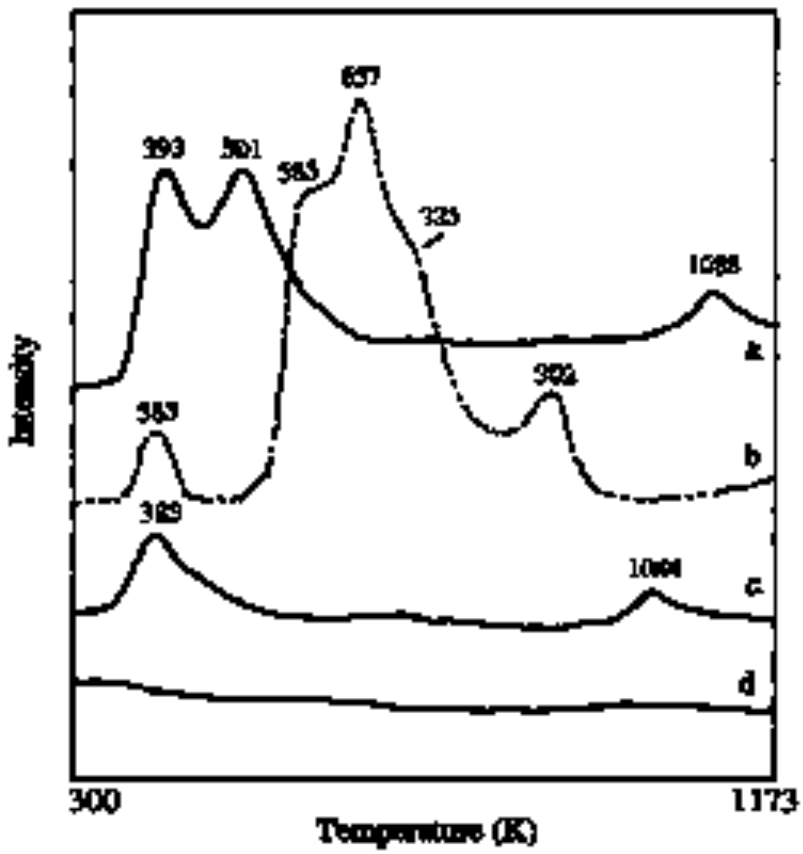

Fig. 1. TPD spectra of Py-adsorbed: a) CeO_2, b) Pr_6O_{11}, c) Tb_4O_7 and d) BaF_2/CeO_2 (Ba/Ce=4), BaF_2/Pr_6O_{11} (Ba/Pr=3), BaF_2/Tb_4O_7 (Ba/Tb=3) catalysts.

657, 725 and 902 K, which could also be attributed to the different acidic centers, respectively. On the surface of pure Tb_4O_7, a weak and a strong acidic site could also be detected. By contrast, almost no Py desorption peak was detected on the BaF_2-promoted catalysts, indicating that their acidities are very weak.

As shown in Fig. 2, only a strong CO_2 desorption peak at 403 K was detected on the surface of CeO_2, indicating that its basic strength is weak. Two CO_2 desorption peaks at 389 and 645 K as well as a shoulder at 595 K were, however, observed on Pr_6O_{11} sample. This suggests that Pr_6O_{11} is a medium strong base with three different basic centers. On the Tb_4O_7 sample, a weak CO_2 desorption peak at 583 K corresponding to a weak basic site was detected. In comparison, the basicities of the BaF_2-promoted catalysts are also very weak, as supported by the TPD results that almost no CO_2 desorption peak was found on the catalysts.

It is well known that most OCM catalysts are basic oxides, the basicity appears to be one of the most fundamental properties of an OCM catalyst for a better C_2 selectivity [2]. However, there are also some effective OCM catalysts, such as

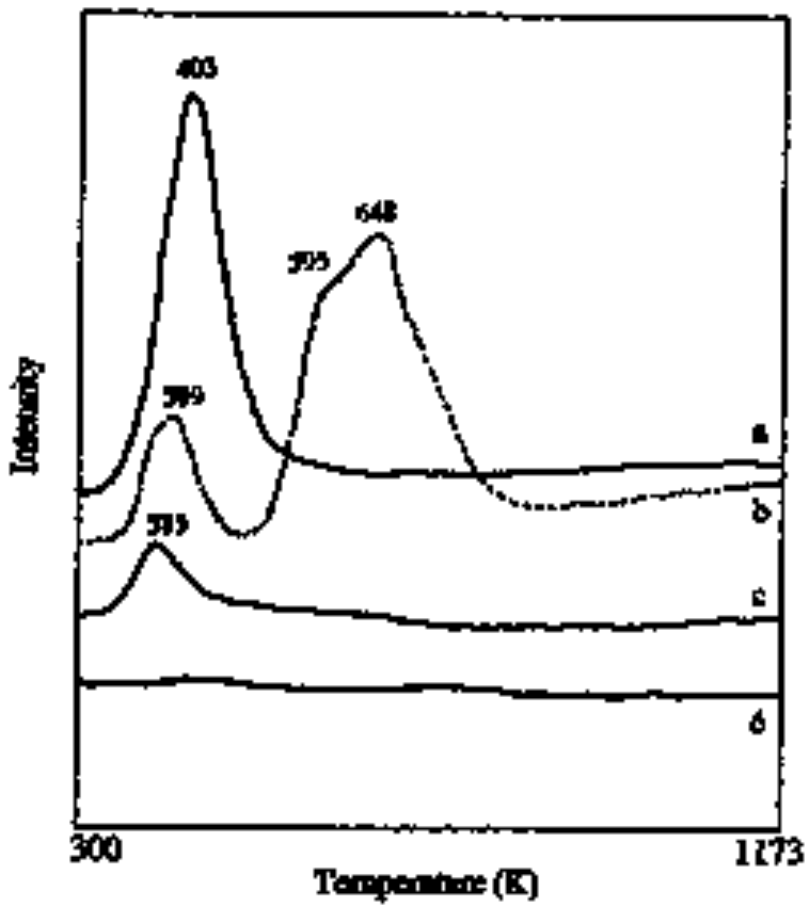

Fig. 2. The TPD spectra of CO_2-adsorbed: (a) CeO_2, (b) Pr_6O_{11}, (c) Tb_4O_7 and (d) BaF_2/CeO_2 (Ba/Ce=4), BaF_2/Pr_6O_{11} (Ba/Pr=2), BaF_2/Tb_4O_7 (Ba/Tb=2) catalysts.

Li/MgCl [28], $Mn/Na_2WO_4/SiO_2$ [29], etc., whose basicities were found to be very weak. The addition of BaF_2 to the multicomponent rare earth oxides caused a sharp decrease in both acidity and basicity, which might be related to the fact that their surfaces are covered with a large amount of BaF_2 that shows neither acidity nor basicity. From the comparison of surface acidity/basicity with catalytic performance of the catalysts, it could be concluded that there was no direct relationship between them.

3.5. Reducibility

TPR spectra for the CeO_2 and BaF_2/CeO_2 samples are shown in Fig. 3. For pure CeO_2, two peaks were observed at approximately 718 and 1117 K. The TPR spectrum can be interpreted as a stepwise reduction of CeO_2. The peak at 718 K

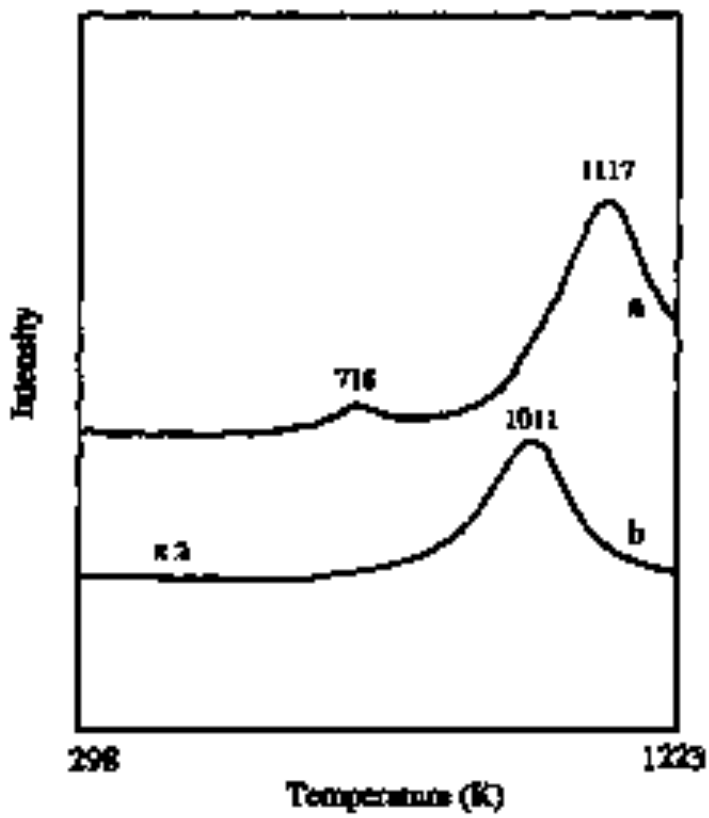

Fig. 3. The TPR spectra of: (a) CeO_2 and (b) BaF_2/CeO_2 (BaF_2/CeO_2=4) catalysts.

amounts to a small percentage of the total area, and it is reasonable to assign this peak to a surface reduction of CeO_2 that has a small BET area [30]. The second peak at 1117 K is attributed to the total reduction of ceria to Ce_2O_3 [30]. The TPR spectrum of BaF_2/CeO_2 showed only a broad peak at 1011 K, which may be assigned to the total reduction of CeO_2 to Ce_2O_3. Since the catalyst surface was covered by a large amount of BaF_2 (XPS result), the reduction of the surface oxygen could not be observed by TPR. The reduction temperature of the bulk oxygen in the BaF_2/CeO_2 sample was found to decrease as compared with pure CeO_2.

The TPR spectra of the Pr_6O_{11} and BaF_2/Pr_6O_{11} are shown in Fig. 4. Two peaks at 766 and 853 K were observed on Pr_6O_{11} sample, which could probably be associated with the reduction of the surface and bulk oxygen of Pr_6O_{11}, respectively. The color of praseodymium oxide reduced was changed to light yellow–green from black, indicating that praseodymium oxide had been reduced to Pr_2O_3 [31]. For the BaF_2/Pr_6O_{11} sample, only a very weak peak at 423 K was observed, which might result from the reduction of surface oxygen adspecies. No phenomenon of the reduction of the surface and bulk lattice oxygen was detected. This is

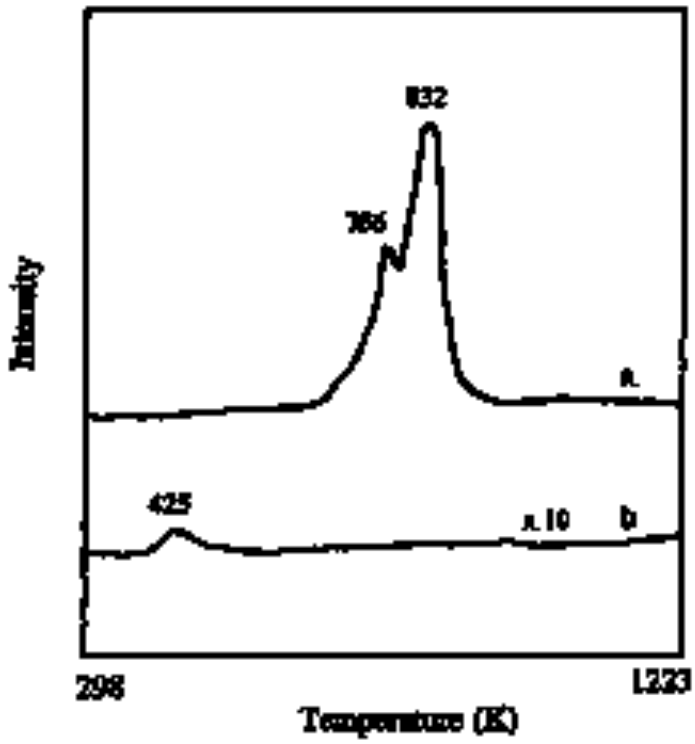

Fig. 4. The TPR spectra of: (a) Pr_6O_{11} and (b) BaF_2/Pr_6O_{11} (Ba/Pr=2) catalyst.

consistent with the above XRD result that most Pr_6O_{11} was converted to undecidable PrOF in the process of the catalyst preparation.

As shown in Fig. 5, two peaks at 768 and 872 K due to the reduction of surface and bulk oxygen, respectively, were detected on the Tb_4O_7 sample. In comparison, it could also be found that two reduction peaks at 761 and 915 K appeared on the BaF_2/Tb_4O_7 catalyst, which could be attributed to the reduction of surface and bulk oxygen, respectively, but the reduction temperatures of the latter clearly increased.

In the process of TPR of oxides, oxygen ions may be removed by inward diffusion of hydrogen or outward diffusion of oxygen ions from oxides to the reaction interface, so the mobility of lattice oxygen and the concentration of oxygen vacancies in oxides will play an important role. From the above TPR results, one can find that, for pure CeO_2, Tb_4O_7 and Pr_6O_{11}, the differences of reduction temperature between surface oxygen and bulk oxygen were 209, 104 and 66 K, respectively. This can be well interpreted by the idea that, with the increase of the conductivity from Ce and Tb to Pr in these oxides [16], the mobilities of lattice oxygen may also increase, resulting in a lower reduction temperature of bulk lattice oxygen. When BaF_2 was added to CeO_2, more anionic vacancies might be produced due to the interaction between them (XRD result), leading to an increase

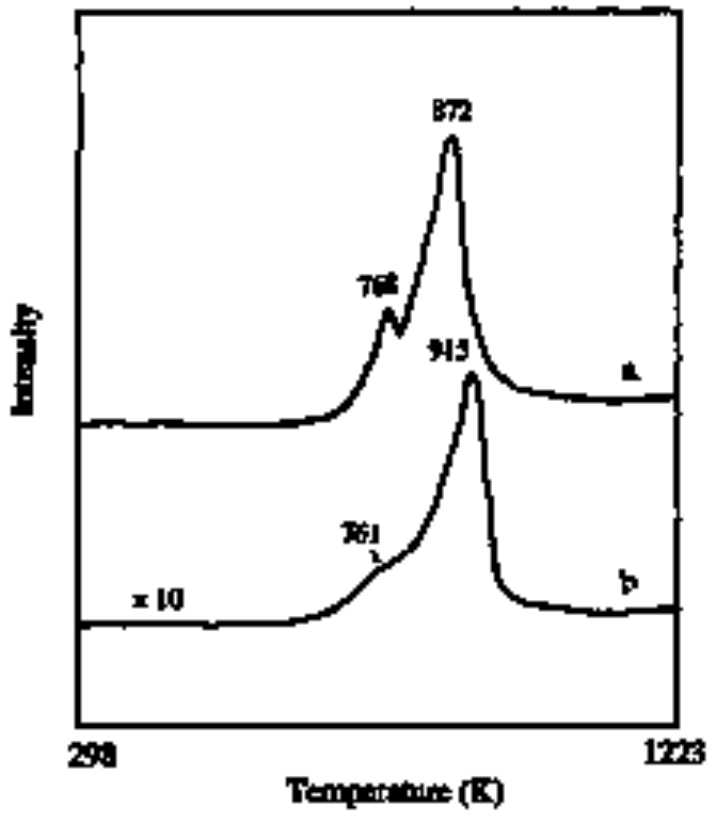

Fig. 5. The TPR spectra of: (a) Th_4O_7 and (b) BaF_2/Th_4O_7 (Ba/Th=2) catalysts.

of the mobility of lattice oxygen and thus to the decrease of the reduction temperature of bulk lattice oxygen. However, since a large amount of oxygen vacancies exist in the cubic Th_4O_7 lattice, the partial substitution of O^{2-} by F^- in BaF_2 (XRD result) may result in a decrease of oxygen vacancies. This will lead to an increase of the reduction temperature of bulk lattice oxygen.

Since the reducible oxygen species on these multivalent rare earth oxides may be responsible for the methane activation, leading to methyl radicals, and also for the further surface oxidation of these methyl radicals to CO_2 [8], the decrease of their concentrations will decrease the chance of deep oxidation of methyl radicals and C_2 hydrocarbons in OCM reaction and thus lead to an increase of C_2 selectivity.

4. Conclusions

It is evident from this study that methane conversions and C_2 selectivities over BaF_2-promoted CeO_2, Pr_6O_{11} and Th_4O_7 catalysts were significantly higher than

those over corresponding oxides under the same conditions of 1073 K, CH_4:02=3:1 and GHSV=20 000 h^{-1}. In the process of catalyst preparation, the partial ion exchange took place, leading to the contraction of BaF_2 lattice and/or the formation of rare earth oxyfluorides. After adding BaF_2 to the rare earth oxides, the concentrations of quadrivalent rare earth ions and reducible oxygen species as well as specific surface area of the catalysts were found to decrease. In addition, the dispersion of F^- on the surface of catalysts will also be helpful for the isolation of the surface active centers. All of these will be favorable to decreasing the chance of deep oxidation of aldehyde radicals and C_2 hydrocarbons and thus resulting in an increase of C_2 selectivity. Since there is a certain correlation between methane conversion and C_2 selectivity for an oxygen-limited OCM reaction, methane conversion will increase along with the increase of C_2 selectivity. However, no direct relationship between the surface acidity/basicity and catalytic activity/selectivity was observed over the catalysts.

Acknowledgements

This work is supported by the National Nature Science Foundation of China.

References

[1] G.E. Keller and M.M. Bhasin, J. Catal., 73 (1982) 9.
[2] A.M. Maitra, Appl. Catal. A, 104 (1993) 11.
[3] K. Otsuka, K. Jinno and A. Morikawa, Chem. Lett. (1985) 499.
[4] K.D. Campbell, H. Zhang and J.H. Lunsford, J. Phys. Chem., 92 (1988) 750.
[5] J.H. Lunsford, Catal. Today 6 (1990) 3.
[6] S. Lacombe, C. Geantet and C. Mirodatos, J. Catal., 151 (1995) 439.
[7] A.M. Gaffney, C.A. Jones, J.J. Leonard and J.A. Sofranko, J. Catal., 114 (1988) 422.
[8] M.G. Poirier, R. Breault, S. Kaliaguine and A. Adnot, Appl. Catal., 71 (1991) 103.
[9] R. Yu, Y. Yang, J.H. Lunsford and M.P. Rosynek, J. Catal., 154 (1995) 163.
[10] S. Sugiyama, Y. Matsumura and J.B. Moffat, J. Catal., 139 (1993) 338.
[11] X.P. Zhou, W.D. Zhang, H.L. Wan and K.R. Tsai, Catal. Lett., 21 (1993) 113.
[12] X.P. Zhou, K.Q. Zhou, W.D. Zhang, Z.S. Chao, W.Z. Weng, R.Q. Long, D.L. Tang, S.Y. Wang, S.J. Wang, J.X. Cai, H.L. Wan, K.R. Tsai, Preprints, Division of Petroleum Chemistry, Inc. ACS, 39 (2), 1994, p. 222.
[13] X.P. Zhou, Z.S. Chao, W.Z. Weng, W.D. Zhang, S.J. Wang, H.L. Wan and K.R. Tsai, Catal. Lett., 29 (1994) 177.
[14] R.Q. Long, S.Q. Zhou, Y.P. Huang, W.Z. Weng, H.L. Wan and K.R. Tsai, Appl. Catal. A, 133 (1995) 269.
[15] J.M. DeBoy and R.F. Hicks, Ind. Eng. Chem. Res., 27 (1988) 1577.
[16] Physics and Chemistry Constants of Rare Earth (China), Edited by Department of Metal in Zhongshan University, Metallurgical Industry Publishing House, 1978, p. 31.
[17] K.A. Gschneidner, Jr., L. Eyring (Eds.), Handbook on the Physics and Chemistry of Rare Earths, vol. 5, North-Holland, 1982, Chap. 41, p. 331.
[18] K. Hikima and S. Yajima, Bull. Chem. Soc. Jpn. 40 (1977) 445.
[19] [illegible], J. Phys., 6 (1994) [illegible].
[20] Handbook of X-ray Photoelectron Spectroscopy, Perkin-Elmer corporation, 1979.
[21] M.F. Hodge and M. Ayyoob, Surf. Sci., 177 (1986) L953.
[22] S. Sugiyama, T. Oshida, K. Sekizawa, H. Hayashi and J.B. Moffat, Bull. Chem. Soc. Jpn., 67 (1994) 3350.

[23] J.L. Dubois, M. Bisiaux and H. Mimoun, Catal. Lett., (1990) 967.
[24] M. Ayyoob and M.S. Hedge, Surf. Sci., 133 (1983) 516.
[25] R.Q. Long, Y.P. Huang and H.L. Wan, J. Raman Spectrosc., 28 (1997) 29.
[26] R.Q. Long and H.L. Wan, J. Chem. Soc., Faraday Trans., 93 (1997) 355.
[27] Y. Tong and J.H. Lunsford, J. Am. Chem. Soc., 113 (1991) 4741.
[28] J.H. Lunsford, P.G. Hinson, M.P. Rosynek, C. Shi, M. Xu and X. Yang, J. Catal., 147 (1994) 301.
[29] X. Fang, S. Li, J. Lin, J. Gu and D. Yan, J. Molec. Catal. (China), 6 (1992) 255.
[30] J.Z. Shyu, W.H. Weber and H.S. Gandhi, J. Phys. Chem., 92 (1988) 4964.
[31] R.E. Ferguson, E.D. Guth and L. Eyring, J. Am. Chem. Soc., 76 (1954) 3890.